

5.7. Summit, Greenland (01/20/14 – 11/24/14)

This section describes quality control of “Volume 24” solar data recorded by the SUV-150B spectroradiometer and the collocated GUV-511 radiometer at Summit Camp, Greenland, between 01/20/14 and 11/23/14.

Periodic changes in responsivity of the SUV-150B spectroradiometer observed during the last years continued in 2014. These changes are caused by variations in collector efficiency and PMT sensitivity. The changes are now well understood and were corrected during data processing. Residual variations in published data were assessed by comparing SUV-150B data with measurements of the GUV-511 multi-filter radiometer and results of radiative transfer calculations, and are smaller than $\pm 2\%$.

Measurements of the TSI sensor internal to the SUV-150B were not always correctly recorded. Defective data were removed from the published databases.

The Eppley pyranometer co-installed with the SUV-150B had the serial number 33120F3 and had been calibrated by Eppley Laboratories on 4/15/2013; the calibration constant is $8.44 \times 10^{-5} \text{ V}/(\text{W m}^{-2})$.

The collectors of the SUV-150B and GUV-511 were shaded by nearby obstacles during some scans. Shading events occurred mostly between 8:30 and 9:00 from mid-April to mid-July. Affected scans were not removed from the Version 0 dataset; however, they were flagged in the Version 2 dataset and mostly removed from the GUV dataset.

A total of 18,102 SUV-150B scans are part of the Summit Volume 24 dataset.

5.7.1. Irradiance Calibration

The on-site irradiance standards used during the reporting period were the lamps 200W027, 200W030, and 200W038. No comparison with a long-term standard took place during the reporting period.

Calibration history of on-site standards 200W027, 200W030, and 200W038

Lamp 200W027 was originally calibrated on 3/28/01 by Optronic Laboratories. The lamp was recalibrated against the project’s traveling standard, lamp 200W017, using “closing” scans performed at Summit on 7/11/07. The lamp was temporarily moved to San Diego and was recalibrated in March 2008 against lamps 200W028 and 200W022. It was recalibrated again in November 2011 against standards 200W017 and 200W038. This calibration was used for processing of solar data of the Volume 21 (2011), Volume 22 (2012), Volume 23 (2013), and Volume 24 (2014) periods.

Lamp 200W030 was originally calibrated on 3/28/01 by Optronic Laboratories. The lamp was recalibrated against lamp 200W017 using “closing” scans performed at Summit on 7/11/07. The lamp was recalibrated in June 2009 against 200W017 using “closing” scans of the Volume 18 period. The lamp was recalibrated again in November 2011 against the traveling standards 200W017 and 200W038. This calibration was used for processing of solar data of the Volume 21 (2011), Volume 22 (2012), and Volume 23 (2013), and Volume 24 (2014) periods.

Lamp 200W038 was calibrated against lamps 200W028 and 200W022 in April 2008. At this time, the calibration of lamp 200W038 was consistent to that of 200W017.

Figure 5.7.1 compares the scales of irradiance of the on-site standards 200W027, 200W030, and 200W038 with each other. The comparison is based on absolute scans performed on 7/3/2014. At that time, the scales agreed to within $\pm 1\%$. The three lamps were also compared on 2/12/14 and 11/5/14 with similar results.

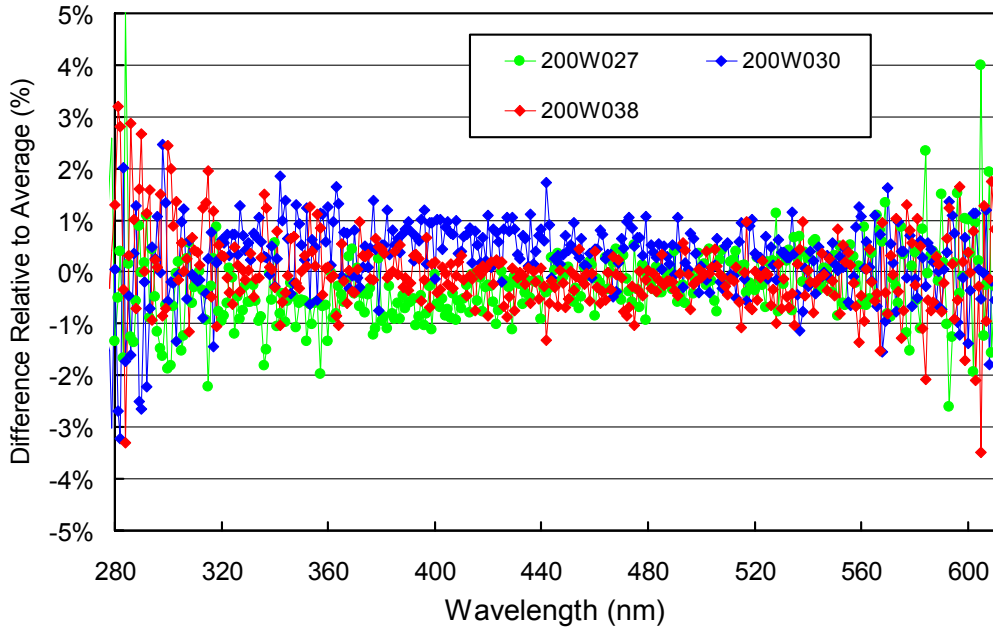


Figure 5.7.1. Comparison of on-site standards 200W027, 200W030, and 200W038 on 7/3/2014.

5.7.2. Instrument Stability

The temporal stability of the spectroradiometer is monitored with bi-weekly calibrations utilizing the on-site standards; daily response scans of the internal irradiance reference lamp; and by comparison with the co-located GUV-511 radiometer and results from a radiative transfer model.

Internal to the instrument's fore optics is a filtered photo diode, called TSI, with a peak sensitivity in the UV. It is used to track changes in the light intensity of the internal reference lamp. By monitoring the TSI while measuring the current of the system's photomultiplier tube (PMT) detector, changes in the lamp's output can be decoupled from drifts in monochromator throughput or PMT sensitivity. Figure 5.7.2 shows changes in TSI readings and PMT currents at 320 and 400 nm, derived from response scans performed between 2/14/06 and 12/21/14. TSI measurements changed by about 10% between 2/14/06 and 6/20/09. The lamp failed at the end of August 2009 and was replaced. Data recorded after this time were scaled downward by a constant factor to better compare with previous measurements. The relative change of the second lamp's intensity as recorded by the TSI between 9/2/09 and 12/21/14 is similar to that of the original lamp, except for the brief period of 7/15/13 – 9/29/13. The trend of PMT currents follows that of the TSI measurements but there is a sinusoidal variation with a periodicity of one year superimposed on the general trend. The highest PMT sensitivity is observed in mid-February of every year, while the lowest sensitivity is observed in August. We attribute this periodicity to a long-term memory of the PMT to the radiation levels it has "seen" during the months prior to the measurement. During the period of winter darkness, the PMT becomes more sensitive, and during the summer months its sensitivity decreases. As the variation is very predictable, it can be well corrected when solar data are processed.

To account for the combined changes of the throughput of the system's entrance optics and PMT-sensitivity, the reporting period was broken into 9 sub-periods and a different irradiance spectrum was applied to the internal lamp in each period. Irradiance spectra were smoothed with an approximating spline to reduce the effect of measurement noise. A summary of the calibration periods is provided in Table 5.7.1. The ratios of irradiance spectra applied in Periods P1 – P8 relative to the spectrum applied in Period P1 are shown in Figure 5.7.3.

The quality of calibrated solar measurements of the SUV-150B was further assessed by comparison with

the GUV-511 radiometer. Figure 5.7.4 shows the ratio of measurements of the GUV's 340 nm channel to measurements of the SUV-150B. The latter have been weighted with the spectral response function of the GUV's channel prior to forming the ratio. Measurements of the two instruments generally agree to within $\pm 5\%$, with the exception of several outliers. The ratio tends to be somewhat lower early and late in the year and is highest during the summer. Most outliers occur between June and August and are related to obstacles in the field of view of either the GUV or the SUV that shade the direct Sun. Because the two instruments are located approximately one meter apart, they are shaded at slightly different times, leading to variations in the ratio. Affected data have been flagged in the SUV Version 2 dataset, but not in the SUV Version 0 dataset.

Table 5.7.1. Calibration periods for Summit Volumes 24.

Period name	Period range	Number of absolute scans	Remarks
P1	01/01/14 – 02/20/14	4	
P2	02/21/14 – 04/12/14	4	
P3	04/13/14 – 04/28/14	0	
P3B	04/29/14 – 05/03/14	1	Average of P3 and P4
P4	05/04/14 – 06/11/14	3	
P5	06/12/14 – 08/20/14	6	
P6	08/21/14 – 10/01/14	3	
P7	10/02/14 – 11/13/14	4	
P8	11/14/14 – 12/31/14	2	

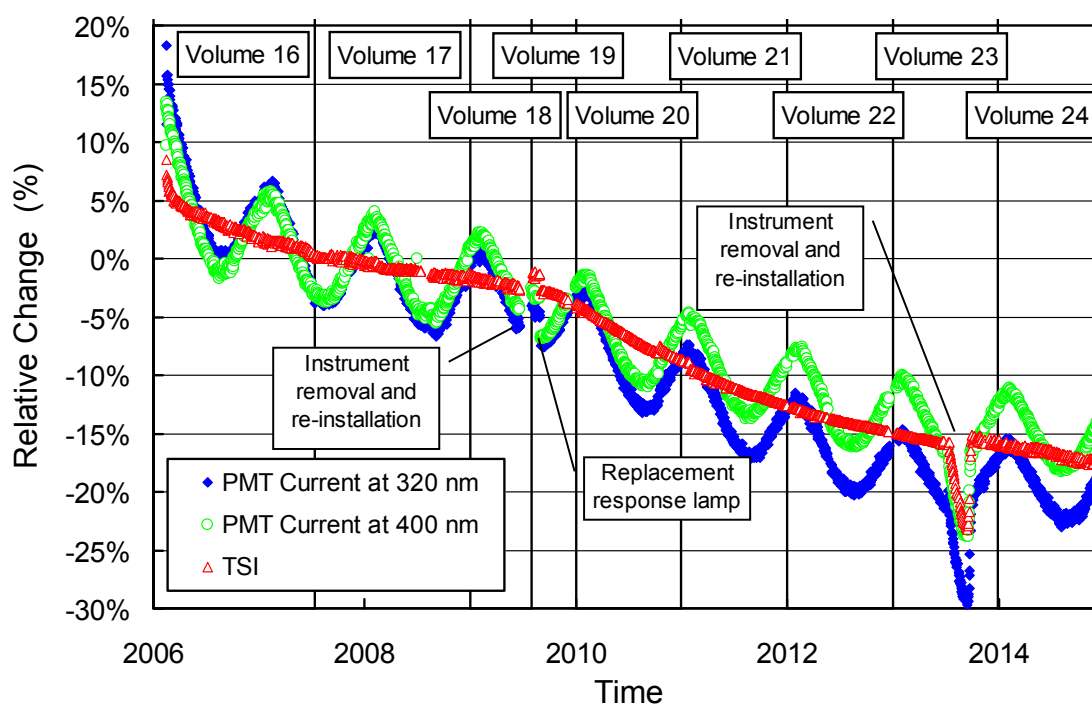


Figure 5.7.2. Time-series of TSI signal and PMT currents at 320 and 400 nm during measurements of the internal reference lamp performed at Summit between 2/15/06 and 12/21/14. Data from 9/2/10 (date of response lamp replacement) were scaled downward to fit into the existing pattern. Data are normalized to the period 2/14/06 - 6/20/09.

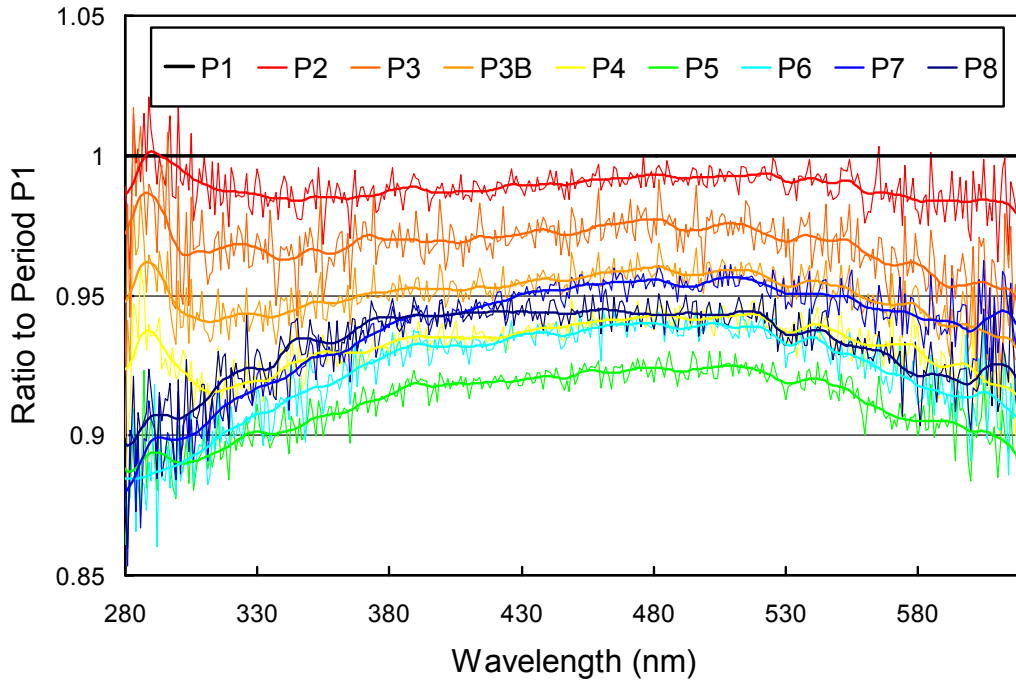


Figure 5.7.3. Ratios of irradiance assigned to the internal reference lamp in Periods P1 – P8, referenced to the irradiance of Period P1. Thick lines indicate ratios of the smoothed irradiance spectra used for the calibration of solar measurements.

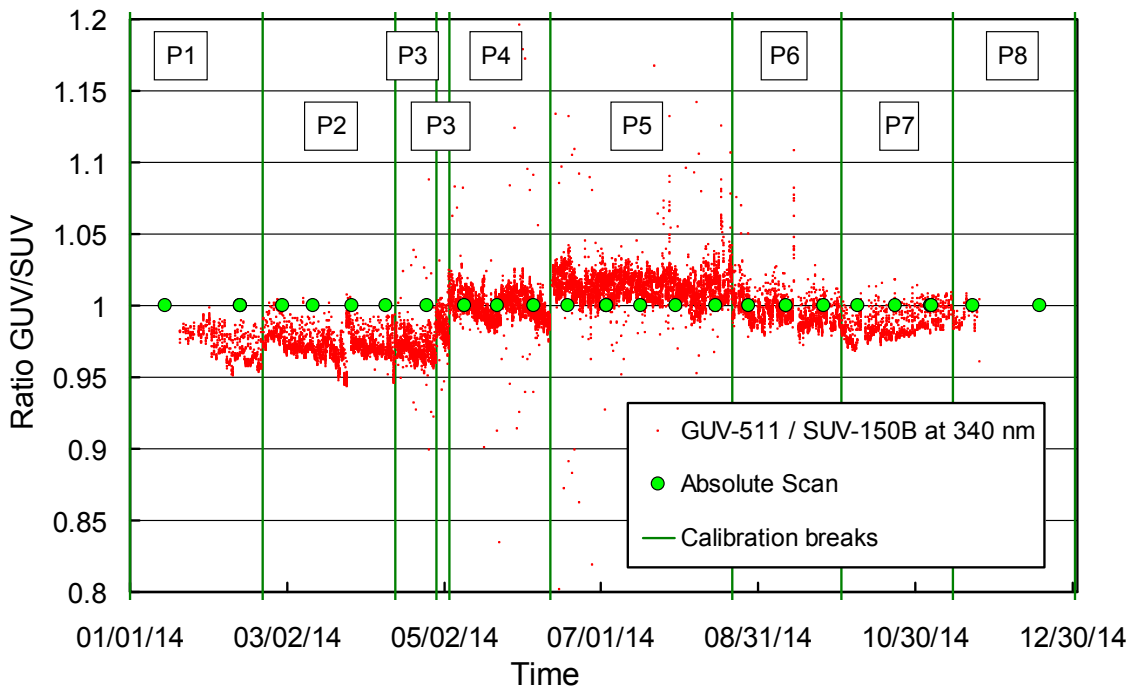


Figure 5.7.4. Ratios of GUV-511 and SUV-150B measurements at 340 nm.

5.7.3. Wavelength Calibration

Wavelength stability of the system was monitored with the internal mercury lamp. Figure 5.7.5 shows the differences in the wavelength offset of the 296.73 nm mercury line between pairs of consecutive wavelength scans for the period 1/1/14 – 12/21/14. 322 scans were evaluated. For 99.4% of the scans is the difference in the wavelength offset to neighboring scans less than ± 0.0055 nm. Minimum and maximum shifts between consecutive scans were -0.008 and +0.007 nm, respectively. Note that the wavelength stability of the system is a factor of 10 better than that of SUV-100 spectroradiometers used at other sites. The SUV-150B has superior stability due to the use of high-resolution optical encoders that are used in a closed feedback loop with the stepper-motor controllers.

After the data were corrected for day-to-day wavelength fluctuations, the wavelength-dependent bias between this homogenized data set and the correct wavelength scale was determined with the Fraunhofer-line correlation method used for Version 2 processing (Bernhard *et al.*, 2004; see also Section 4.2.2.2). Due to the good wavelength stability of the system, only one correction function had to be applied for the entire reporting period (Figure 5.7.6). Since the position of the monochromator's gratings is determined by optical encoders, irregularities in the monochromator drive are inconsequential. This explains the smoothness of the functions.

After data was corrected using this function, the wavelength accuracy of all noontime scans was verified with the "Version 2" Fraunhofer-line correlation algorithm. Results are shown in Figure 5.7.7. Residual wavelength errors are smaller than ± 0.03 nm, with few exceptions.

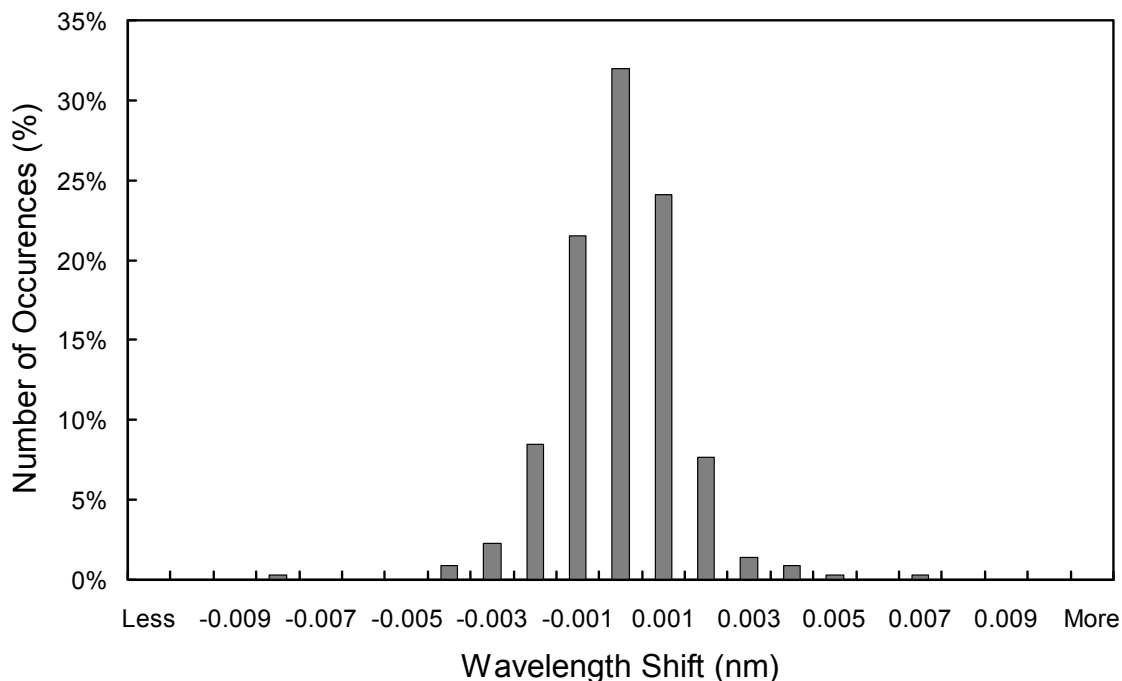


Figure 5.7.5. Differences in the measured position of the 296.73 nm mercury line between consecutive wavelength scans for the period 1/1/14 – 12/21/14. The labels of the horizontal axis give the center wavelength shift for each column. The 0-nm histogram column covers the range from -0.0005 to +0.0005 nm. “Less” means shifts smaller than -0.0105 nm; “more” means shifts larger than 0.0105 nm.

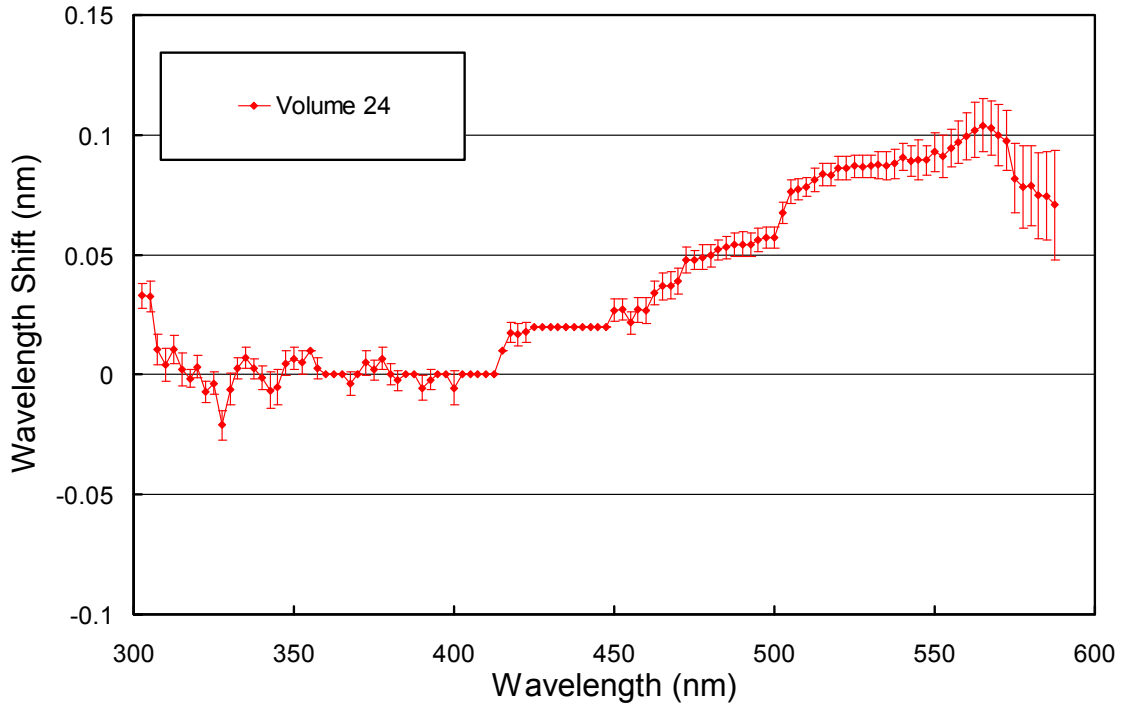


Figure 5.7.6. Monochromator non-linearity correction functions of Volume 24 data.

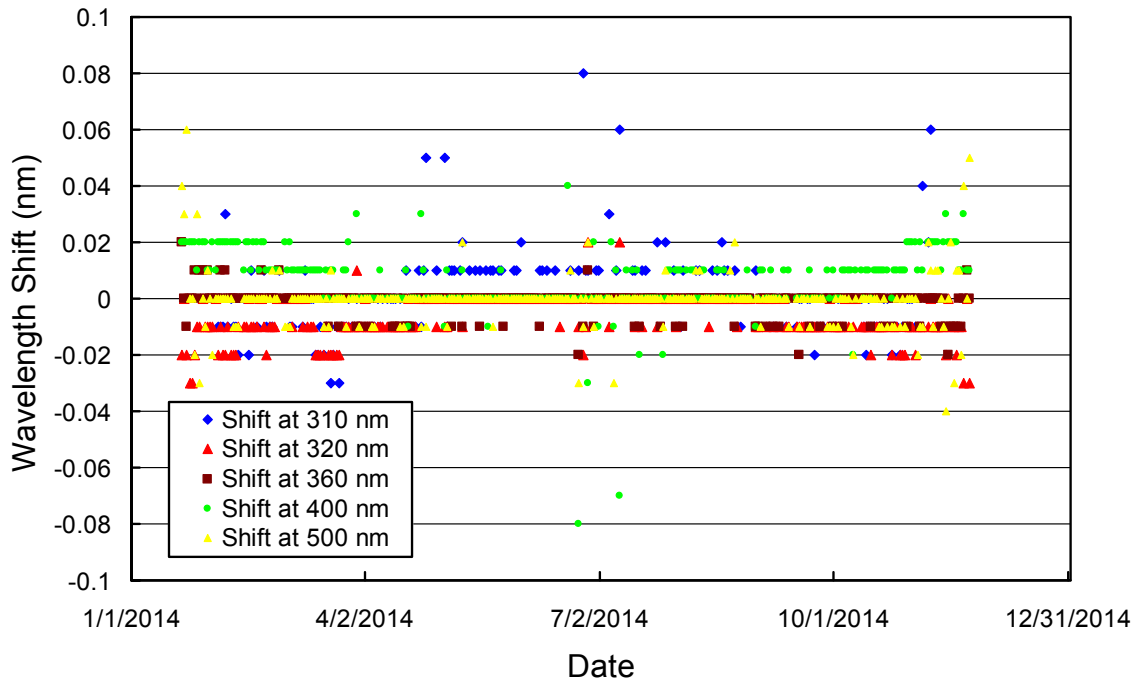


Figure 5.7.7. Wavelength accuracy check of "Version 0" Volume 24 data at five wavelengths in the UV and visible by means of Fraunhofer-line correlation. All noontime measurements have been evaluated.

5.7.4. Missing Data

A total of 18,102 scans are part of the Summit Volume 24 dataset. Missing periods are summarized in Table 5.7.2.

Table 5.7.2. Incomplete days in the Summit Volume 24 dataset.

Period	Reason
04/09/14	Communication to system's electrometer severed.
06/10/14	Operator error
08/22/14 – 08/23/14	Problem communicating with the shutter of the system
08/30/14	unknown
09/14/14 – 09/15/14	Software error ("error 91")
09/27/14	Software error ("error 91")
10/10/14 – 10/11/14	Software error ("error 91")
11/05/14	Triple absolute scan

5.7.5. GUV Data

The GUV-511 radiometer installed next to the SUV-150B was calibrated against SUV-150B measurements following the procedure outlined in Section 4.3.1. From the calibrated measurements, data products were calculated (Section 4.3.2). Figure 5.7.8 shows a comparison of GUV-511 and SUV-150B erythemal irradiance for the Volume 24 period. For solar zenith angles (SZA) smaller than 80°, measurements of the two instruments agree to within $\pm 2.0\%$ ($\pm 1\sigma$). We advise data users to use SUV-150B rather than GUV-511 data whenever possible, in particular for low-Sun conditions.

Figure 5.7.9 shows a comparison of total ozone measurements from the GUV-511, SUV-150B (Version 2), and Ozone Monitoring Instrument (OMI). The SUV-150B data agree well with OMI observations, except for the period 3/13/14 - 3/22/14 when some OMI measurements are considerably larger. It appears that OMI measurements during this period are biased high at times when the solar zenith angle is larger than 80°. A large zenith angle during a period of high ozone results in a small signal back-scattered to space.

The average ratio SUV/OMI is 0.9964, and the standard deviation of the ratio is 2.0%. This good agreement—even at large SZAs—is achieved by using ozone profiles in the inversion algorithm, which were measured at Summit by NOAA's Global Monitoring Division close in time to the UV observations. The average ratio GUV / OMI for SZAs smaller than 80° is 1.004 and the standard deviation of the ratio is also 2.0%. However, GUV measurements systematically underestimate the true ozone column between March and mid-April. The calculation of total ozone from GUV data is based on one standard ozone profile via a lookup table, which may not be appropriate in the spring when the total ozone column is large. Because of this profile effect, GUV measurements tend to be too small in the spring, in particular if the SZA is large. For solar zenith angles larger than 80°, measurements of the GUV's 305 nm channel are close to the detection limit. GUV ozone data at large SZAs become unreliable and should not be used.

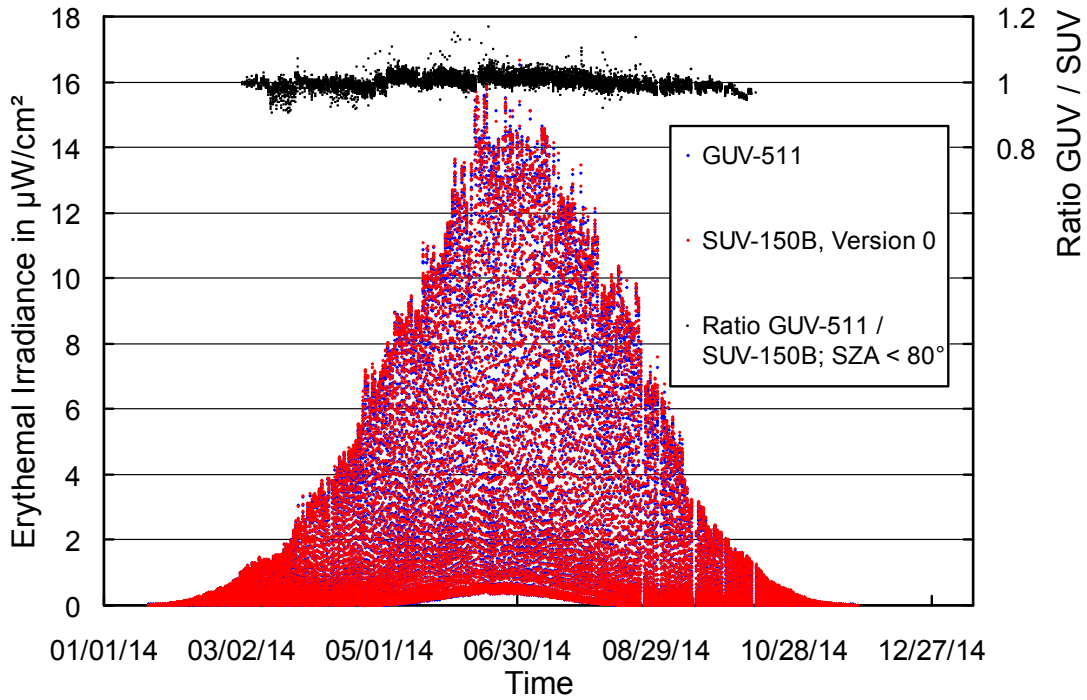


Figure 5.7.8. Comparison of erythemal irradiance measured by the SUV-150B spectroradiometer and the GUV-511 radiometer.

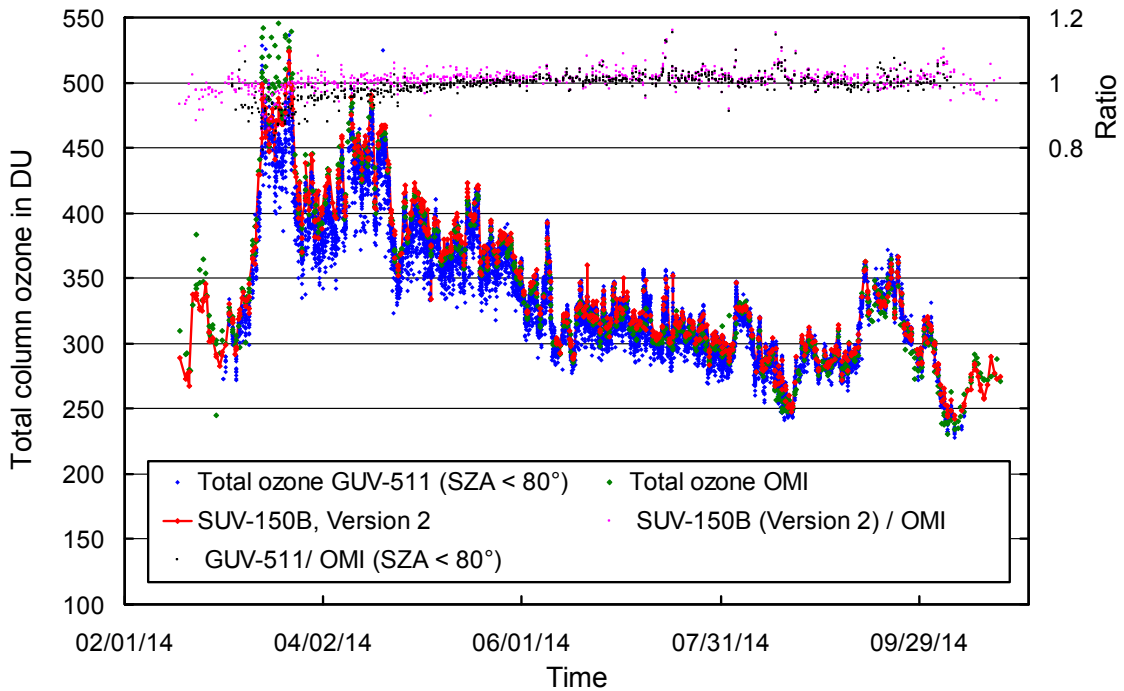


Figure 5.7.9. Comparison of total column ozone measurements from GUV-511, SUV-150B (Version 2 data), and OMI. GUV-511 measurements are plotted in 15 minute intervals. For calculating the ratio of data sets, only measurements concurrent with the OMI overpass were evaluated.